

Effects of local meteorology and aerosols on ozone and nitrogen dioxide retrievals from OMI and pandora spectrometers in Maryland, USA during DISCOVER-AQ 2011

Andra J. Reed · Anne M. Thompson ·
Debra E. Kollonige · Douglas K. Martins ·
Maria A. Tzortziou · Jay R. Herman ·
Timothy A. Berkoff · Nader K. Abuhassan ·
Alexander Cede

Received: 19 November 2012 / Accepted: 19 March 2013 /
Published online: 19 April 2013
© The Author(s) 2013. This article is published with open access at Springerlink.com

Abstract An analysis is presented for both ground- and satellite-based retrievals of total column ozone and nitrogen dioxide levels from the Washington, D.C., and Baltimore, Maryland, metropolitan area during the NASA-sponsored July 2011 campaign of *Deriving Information on Surface COnditions from Column and VERTically Resolved Observations Relevant to Air Quality* (DISCOVER-AQ). Satellite retrievals of total column ozone and nitrogen dioxide from the Ozone Monitoring Instrument (OMI) on the Aura satellite are used, while Pandora spectrometers provide total column ozone and nitrogen dioxide

A. J. Reed (✉) · A. M. Thompson · D. E. Kollonige · D. K. Martins
Department of Meteorology, The Pennsylvania State University,
University Park, PA, USA
e-mail: axr5145@psu.edu

M. A. Tzortziou
Earth System Science Interdisciplinary Center, University of Maryland,
College Park, MD, USA

M. A. Tzortziou · J. R. Herman · N. K. Abuhassan · A. Cede
NASA Goddard Space Flight Center, Greenbelt, MD, USA

J. R. Herman
Joint Center for Earth Systems Technology, University of Maryland,
Baltimore County, Baltimore, MD, USA

T. A. Berkoff
Goddard Earth Sciences and Technology Center, University of Maryland,
Baltimore County, Baltimore, MD, USA

N. K. Abuhassan
LuftBlick, Kreith, Austria

A. Cede
School of Engineering, Morgan State University,
Baltimore, MD, USA

amounts from the ground. We found that OMI and Pandora agree well (residuals within $\pm 25\%$ for nitrogen dioxide, and $\pm 4.5\%$ for ozone) for a majority of coincident observations during July 2011. Comparisons with surface nitrogen dioxide from a Teledyne API 200 EU NO_x Analyzer showed nitrogen dioxide diurnal variability that was consistent with measurements by Pandora. However, the wide OMI field of view, clouds, and aerosols affected retrievals on certain days, resulting in differences between Pandora and OMI of up to $\pm 65\%$ for total column nitrogen dioxide, and $\pm 23\%$ for total column ozone. As expected, significant cloud cover (cloud fraction >0.2) was the most important parameter affecting comparisons of ozone retrievals; however, small, passing cumulus clouds that do not coincide with a high (>0.2) cloud fraction, or low aerosol layers which cause significant backscatter near the ground affected the comparisons of total column nitrogen dioxide retrievals. Our results will impact post-processing satellite retrieval algorithms and quality control procedures.

Keywords Ozone Monitoring Instrument (OMI) · Pandora · Total column ozone · Total column nitrogen dioxide · Atmospheric chemistry · DISCOVER-AQ

1 Introduction

In July 2011, NASA began a multi-year “Earth Venture Program” called *Deriving Information on Surface COnditions from Column and VERTically Resolved Observations Relevant to Air Quality* (DISCOVER-AQ). A combination of in situ and remotely-sensed measurements were conducted on board aircraft, satellite, and ground platforms to relate column observations to surface conditions and investigate the temporal and spatial variability of select atmospheric trace gases.

Validation of satellite data and other atmospheric remote sensing data is an ongoing process, as new instruments and algorithms are developed and current instruments age. Satellite validation becomes increasingly important as studies emerge that focus on relating retrieved satellite quantities to measures of trace gases relevant to air quality regulations and forecasting (Chatfield and Esswein 2012; Martins et al. *this issue*). Previous validation studies of total column retrievals of ozone from satellites and ground-based spectrometers have been performed with a focus on instrument characteristics that may result in either agreement or disagreement between instrument retrievals (Celarier et al. 2008; McPeters et al. 2008; Anton et al. 2009; Herman et al. 2009; Hains et al. 2010; Tzortziou et al. 2012). A number of other validation studies in recent years have focused on total column nitrogen dioxide (TCNO₂) retrievals from the Aura Ozone Monitoring Instrument (OMI) and surface instruments (Boersma et al. 2008; Brinksma et al. 2008; Bucsela et al. 2008; Celarier et al. 2008; Wenig et al. 2008; Hains et al. 2010).

Comparisons of OMI Total Ozone Mapping Spectrometer (OMI-TOMS) and OMI Differential Optical Absorption Spectroscopy (DOAS) satellite retrievals of total column ozone (TCO₃) with ground-based instrumentation such as Brewer and Dobson spectroradiometers show that satellite residuals range from -2.0% to 1.4% , and that the differences between the satellite and ground retrievals are seasonally dependent (McPeters et al. 2008; Anton et al. 2009). Similarly, satellite retrievals of TCNO₂ tend to show a low bias ($\sim 25\%$) when compared to boundary layer columns derived from surface measurements, aircraft profiles, and ground-based spectrometers and DOAS instruments (Boersma et al. 2008; Brinksma et al. 2008; Bucsela et al. 2008; Celarier et al. 2008; Wenig et al. 2008; Hains et al. 2010). The satellite

retrieval TCNO_2 residuals from the surface are a function of field of view (FOV) of the satellite spectrometers as well as boundary layer pollution (Celorier et al. 2008).

Recently, validation of OMI satellite TCNO_2 retrievals was conducted using a Pandora ground-based spectrometer system at the Goddard Space Flight Center (GSFC) in Greenbelt, Maryland (Herman et al. 2009). Pandora is a direct-sun, linear array detector spectrometer that can measure absorption spectra at multiple wavelengths simultaneously, providing concurrent retrievals of both O_3 and NO_2 total column amounts from the ground (Herman et al. 2009; Tzortziou et al. 2012), making it an ideal instrument to use in comparisons with OMI data products.

Various studies with Pandora have found that retrievals from the instrument agree well with those from other ground-based instruments. Pandora TCNO_2 retrievals agreed with retrievals from a Fourier Transform Ultraviolet Spectrometer to within 4 % (Herman et al. 2009), and Pandora slant column abundances agree with those from a Multi-function DOAS to within 5 %, with Pandora slant columns being slightly larger (Wang et al. 2010). Additionally, more than 30 different in situ and remote sensing instruments from around the world were gathered at the Royal Dutch Meteorological Institute's (KNMI's) Cabauw Experimental Site for Atmospheric Research (CESAR) from June to July 2009 to determine the accuracy of the various ground-based instruments and investigate their usefulness in satellite validation. Results indicated that MAX-DOAS slant column densities of trace gases from multiple instruments, including Pandora, were obtained with a precision of approximately 5–10 %. Slant column measurements of NO_2 from most of the MAX-DOAS instruments agreed with one another to within about 5 % (Piters et al. 2012). Tzortziou et al. (2012) compared Pandora TCO_3 retrievals with measurements from a well calibrated double-grating Brewer spectrometer over a period of more than a year in Greenbelt MD, and found excellent agreement and a small bias of approximately 2 DU (or, 0.6 %). This agreement was constant with slant column O_3 amounts up to 1,500 DU, indicating adequate Pandora stray light correction. A small (1–2 %) seasonal difference was found, consistent with sensitivity studies showing that the Pandora spectral fitting TCO_3 retrieval has a temperature dependence of 1 % per 3 K, with an underestimation in temperature (e.g., during summer) resulting in an underestimation of TCO_3 .

Tzortziou et al. (2012) also compared OMI TCO_3 retrievals with ground-based measurements from Pandora instruments deployed at four mid-to high-latitude sites in Europe and the United States. Observations showed that Pandora agreed well with OMI, with average residuals of <1 % at the different sites when the OMI view was within 50 km from the Pandora location and OMI-measured cloud fraction was <0.2. The frequent and continuous measurements by Pandora revealed significant short-term temporal changes in TCO_3 , in many cases associated with weather systems (e.g. pressure changes, passage of a cold front with high ozone content, or intrusion of low-ozone air from lower latitudes), which are not possible to capture by sun-synchronous satellites, such as OMI, alone.

The OMI validation study by Herman et al. (2009), comparing OMI and Pandora TCNO_2 , indicated that the satellite FOV has a significant impact on satellite retrievals. It was found that for cases in which the OMI FOV closely coincided with the location of the ground-based spectrometer in a homogeneous environment, there was good agreement between retrievals of TCNO_2 from both Pandora and OMI. However, due to the coarse resolution of OMI, retrievals from OMI in highly polluted regions tend to be biased to low values compared to Pandora because adjacent rural regions are averaged with the targeted polluted area. The impact of the FOV is largely due to the extremely variable nature of tropospheric NO_2 in time and space (Herman et al. 2009).

The discrepancies between satellite-and ground-based retrievals caused by spatial variation indicate the need for more rigorous data collection for comparison of OMI and ground based instrument retrievals across a heterogeneous region (Celarier et al. 2008; Herman et al. 2009). This study utilizes measurements collected during DISCOVER-AQ in July 2011 in the Washington, D.C. and Baltimore, MD metropolitan regions (Fig. 1). Deployment of Pandora spectrometers at multiple sites within an urban air-shed provides information on short-term and small-scale dynamics and variability in trace gases, which is critical for validation of satellite retrievals (Herman et al. 2009; Tzortziou et al. 2012). In this work, the relative responses of the ground- and satellite-based instruments are investigated in the context of atmospheric dynamics and composition. This study reveals that environmental conditions, including varying cloud cover and aerosol layers, affect the two products differently; thus, the days that exhibit the greatest differences between TCO_3 retrievals tend not to be the same days that exhibit the greatest differences between TCNO_2 retrievals from the two instruments.

2 Methods and data

2.1 Total column trace gas amounts

Total column retrievals are taken from OMI, Pandora spectrometers, and ozonesondes (Table 1).

OMI was launched on the NASA Earth Observing System (EOS) Aura satellite in July 2004 (Schoeberl et al. 2006). Aura has a sun-synchronous polar orbit and crosses the equator at approximately 13:45 local time every day. OMI is an ultraviolet/visible nadir spectrograph, and has a spatial resolution of $13\text{ km} \times 24\text{ km}$ at nadir (Levlett et al. 2006). OMI uses a DOAS fit to retrieve NO_2 vertical column amounts (Table 2; Bucsela et al. 2006). Rayleigh

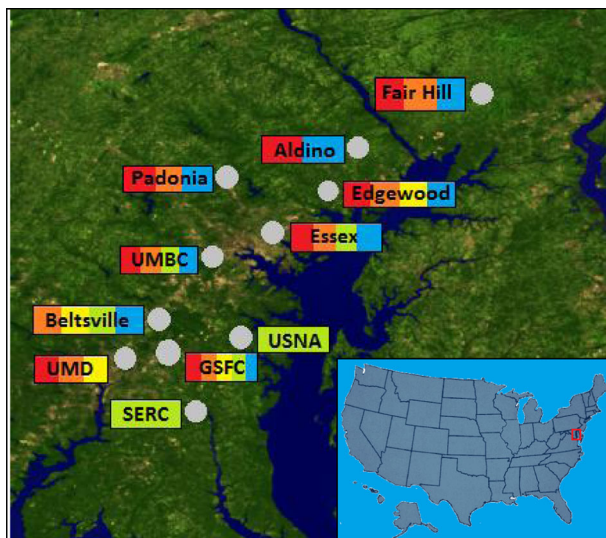


Fig. 1 DISCOVER-AQ 2011 region and ground measurement sites. Colors indicate dates on which the sites saw large differences between both Pandora and OMI TCO_3 retrievals: 8 July (Red), 13 July (Orange), and TCNO_2 retrievals: 15 July (Yellow), 16 July (Green), 26 July (Blue)

Table 1 Summary of instruments and data

Instrument	Data	Origin of data
OMI	Total Column O ₃ , NO ₂	Aura Satellite http://avdc.gsfc.nasa.gov/index.php?site=666843934&id=13
Pandora	Total Column O ₃ , NO ₂	11 Ground Sites throughout the Baltimore, MD and Washington, D.C. region (Fig. 1)
Ozonesondes	Total Column O ₃	Edgewood, MD Beltsville, MD
MODIS	Aerosol Optical Depth (AOD) Visible Images	Aqua Satellite http://disc.sci.gsfc.nasa.gov/giovanni/overview/index.html
MPL	Cloud profiles Aerosol profiles	Edgewood, MD
HYSPLIT	Back Trajectories	NAM12 Model NOAA HYSPLIT
NATIVE	Surface NO, NO _x Total Reactive Nitrogen (NO _y) Photolysis Rate of NO ₂ (j_{NO_2})	Edgewood, MD
MERRA Model	Cloud Liquid Water Content Cloud Top Pressure	GEOS-5 (Goddard Earth Observing System 5) http://disc.sci.gsfc.nasa.gov/giovanni/overview/index.html
CIMEL	AOD	Goddard Space Flight Center in Greenbelt, MD http://aeronet.gsfc.nasa.gov/new_web/system_descriptions_instrument.html

scattering, cloud cover, and aerosols have been accounted for whenever possible in order to provide the best retrievals (Boersma et al. 2002; Chance 2002; Krotkov et al. 2012; Bucsela et al. 2006). To determine TCNO₂ amounts, slant column abundances for both NO₂ and species that interfere with NO₂ absorption, such as N₂O₄, are retrieved by OMI. These slant column abundances are divided by air mass factors, which can be affected by both cloud cover and aerosols in high amounts, to determine the vertical column density. Spatial filtering, including algorithms to determine geographic regions with high NO₂, is then applied to the vertical column densities to yield the final TCNO₂ amount from OMI (Boersma et al. 2002; Bucsela et al. 2006). Based on sensitivity studies, the total expected error in OMI TCNO₂ retrievals is about 5 % in clear, unpolluted conditions, but can be as large as 20–50 % in polluted or cloudy conditions (Boersma et al. 2002; Ionov et al. 2008). The largest sources of errors are the assumptions built into the retrieval algorithm, such as reflectivity and the assumed profile shape, especially when there are large amounts of NO₂ present.

The OMI-TOMS V8.5 O₃ product (Anton et al. 2009; Bhartia and Wellemeyer 2002) is used for TCO₃ comparisons in this study (see Table 2). Cloud cover, aerosols, sea glint, and SO₂ absorption are accounted for in the OMI-TOMS V8.5 algorithm in order to provide the most accurate TCO₃ retrievals. The OMI-TOMS algorithm TCO₃ data have root mean square errors of 1–2 % (Yang and Bhartia 2012).

OMI overpass data from NASA isolate the OMI pixel nearest the ground stations of interest and provide the corresponding TCO₃ and TCNO₂ retrievals for direct comparisons. In addition to the total column amount, OMI overpass data files contain flags for conditions that could cause erroneous retrievals. Included in this information is the UV aerosol index,

Table 2 OMI and Pandora data retrieval information

	OMI NO ₂	OMI O ₃	Pandora NO ₂	Pandora O ₃
Frequency of Retrievals	Once Daily	Once Daily	~ Every 2 min	~ Every 2 min
Resolution	13 km along track x 24 km across track (at nadir)	13 km along track x 24 km across track (at nadir)	1.6° Field of View	1.6° Field of View
Measured Wavelengths	405-465 nm	317.5 nm and 331.2 nm	400-440 nm	305-328.6 nm
Retrieval Method	DOAS	TOMS	DOAS	DOAS
Data Version	Level 2 Overpass Data, Version 3	Level 2 Overpass Data, Version 8.5	UV Aerosol Index >0.5, Distance from center of OMI pixel to measurement site >60 km, Cloud Fraction >0.2	Number of Pandora retrievals in the hour surrounding the OMI overpass <10
Conditions noted in OMI/Pandora Comparisons	OMI Cross Track Position (CTP) <10 or >50, Distance from center of OMI pixel to measurement site >60 km, Cloud Fraction >0.2			Number of Pandora retrievals in the hour surrounding the OMI overpass <10

the distance from the center of the OMI pixel to the ground site, the OMI Cross Track Position, or CTP (which identifies the location of the OMI pixel in the instrument's swath), and the cloud fraction retrieved by OMI (Table 2). OMI overpass data were obtained from the NASA GSFC Aura Validation Data Center (AVDC) (Table 1).

Pandora's algorithms that retrieve ground-based TCO_3 and TCNO_2 amounts use direct-sun irradiances between 280 nm and 525 nm at a resolution of approximately 0.5 nm (Brinksma et al. 2008; Herman et al. 2009; Tzortziou et al. 2012). Pandora has a 1.6° FOV (a circle of ~120 m in diameter at 4 km altitude) and is mounted on a precision pan-tilt tracking device to follow the position of the center of the sun. Pandora retrieves total columns approximately every 2 min. Clouds, ambient temperature, and absorption cross sections all introduce uncertainties into the Pandora TCO_3 and TCNO_2 retrievals, and must be corrected in the instrument's retrieval algorithm (Herman et al. 2009; Tzortziou et al. 2012; Table 2). Absolute error in Pandora retrievals is ± 0.1 DU, with a precision of about ± 0.1 DU in clear skies. This error grows with noise created by clouds in a given retrieval. Pandora TCNO_2 retrievals from the DISCOVER-AQ archives have errors of $\leq 10\%$, and Pandora TCO_3 data used from the DISCOVER-AQ archives have errors of 1–2 %. It should be noted that Pandora TCO_3 data from the Smithsonian Environmental Research Center (SERC) required a 4 % adjustment upwards after the campaign due to calibration issues with the instrument (Tzortziou et al. *this issue*). A network of 11 Pandora spectrometers was distributed across an area of approximately 5,280 km² in central Maryland (spanning approximately 25 pixels of OMI Level 3 data) during the July 2011 DISCOVER-AQ campaign.

TCO_3 was also measured in situ via approximately daily ozonesonde profiles at the Beltsville and Edgewood sites. An ozonesonde is a light-weight, balloon-borne instrument that uses an electrochemical concentration cell (ECC) to quantitatively determine the O_3 partial pressure as it ascends through the atmosphere (Komhyr 1969; Thompson et al. 2003). The average maximum sampling height of the 39 ozonesonde profiles from Edgewood, MD (lat: 39.4100, lon: -76.2967) during the campaign was 32.4 km. TCO_3 is determined from the ozonesonde data with the addition of an above-burst column based on the new climatology of McPeters and Labow (2012). For the Edgewood soundings, the ozone data were corrected to account for a bias in the instrument technique used, as described by Martins et al. (*this issue*). TCO_3 measurements from the ozonesonde have a measurement uncertainty of approximately 9 % (Smit et al. 2007). A detailed discussion of ozonesonde TCO_3 during DISCOVER-AQ, as well as other ozonesonde comparisons, including comparisons to a tropospheric ozone OMI-based product, appears in Thompson et al. (*this issue*).

2.2 Aerosol data

Aerosol data and properties relevant to this study were obtained from the Moderate Resolution Imaging Spectroradiometer (MODIS), a Micro-pulse LIDAR instrument, and a CIMEL sun photometer.

MODIS, on Aqua, crosses the equator at approximately 13:30 local time (Savtchenko et al. 2004) providing data products that are based on measurements performed only 15 min prior to those by Aura OMI. MODIS products used in this study include aerosol optical depth (AOD), as well as cloud optical depth and physical properties (Table 1; Savtchenko et al. 2004). Sources of error in MODIS products include assumptions relating to surface conditions, aerosol properties, and calibration expectations (Remer et al. 2005).

Several Micro-pulse Light Detection and Ranging (LIDAR), or MPL instruments were operated during the DISCOVER-AQ campaign (Table 1). The MPL is a solid state, ground-

based LIDAR instrument used for vertically resolved aerosol detection up to 17 km above the surface (Spinhirne 1993; Berkoff et al. 2003). MPL observations are valuable in the context of this study because both OMI and Pandora retrievals exhibit errors when clouds or significant levels of aerosols are present in the atmosphere.

A CIMEL sun photometer provided retrievals of AOD during the DISCOVER-AQ campaign (Holben et al. 1998; Table 1). CIMEL values of AOD at GSFC are compared here with AOD retrievals from MODIS. The general agreement found between the two instruments for cases in which aerosols are suspected as a cause of differences between Pandora and OMI retrievals increases our confidence in retrievals from both MODIS and CIMEL.

2.3 Meteorological and in situ trace gas data

Temperature, pressure, relative humidity, wind speed, and wind direction measurements were collected by the Maryland Department of the Environment (MDE) and the Nittany Atmospheric Trailer and Integrated Validation Experiment (NATIVE) at Edgewood, MD. NATIVE, a mobile atmospheric research facility, was deployed for the DISCOVER-AQ campaign. Specific instruments on board NATIVE include O_3 , SO_2 , CO, and NO_y analyzers, details of which can be found in Martins et al. (2012). In addition, j_{NO_2} , the radiometer-measured photolysis rate of NO_2 , is obtained from NATIVE instrumentation. During July 2011, the NATIVE payload at Edgewood was supplemented with a Teledyne Advanced Pollution Instrumentation (API) instrument for in situ measurements of NO_x (NO and NO_2) concentrations in the atmosphere.

Analyses using assimilated meteorological data and reanalysis models were conducted. HYSPLIT was combined with NAM12 gridded meteorological data files (Table 1) to provide 24-hour back trajectories for the DISCOVER-AQ sites at heights of 500 m and 1,000 m on the dates of 15, 16, and 26 July 2011. The MERRA Model, developed by the Global Modeling and Assimilation Office at NASA's GSFC, produces meteorological fields using the Global Earth Observing System version 5 (GEOS-5) data assimilation system (Table 1), including satellite radiances and remotely sensed datasets from Television Infrared Observation Satellite (TIROS) Operational Vertical Sounder (TOVS), Advanced TIROS Operational Vertical Sounders (ATOVS), EOS Aqua, Geostationary Operational Environmental Satellite (GOES) Sounders, and the Special Sensor Microwave/Imager (SSM/I) aboard a Defense Meteorological Satellite Program (DMSP) satellite, and observational data from radiosondes, dropsondes, aircraft, and surface stations (Bosilovich 2008). Improvements continue to be made in the MERRA model towards greater agreement with observational data. However, in many fields, the MERRA model compares well with other reanalyses, such as ERA-Interim, or the interim version of the next European Centre for Medium-range Weather Forecasts (ECMWF) Re-Analysis (Rienecker et al. 2011). MERRA model output (Table 1) provides information for analyzing cloud cover, which can cause retrieval errors in the TCO_3 and $TCNO_2$ amounts from the OMI and Pandora instruments.

3 TCO_3

For validation of OMI-TOMS V8.5 TCO_3 , we compare to the Pandora O_3 column at 11 stations, including Edgewood, Maryland (Fig. 2). At NATIVE, in Edgewood, an independent O_3 measurement is obtained from ozonesondes.

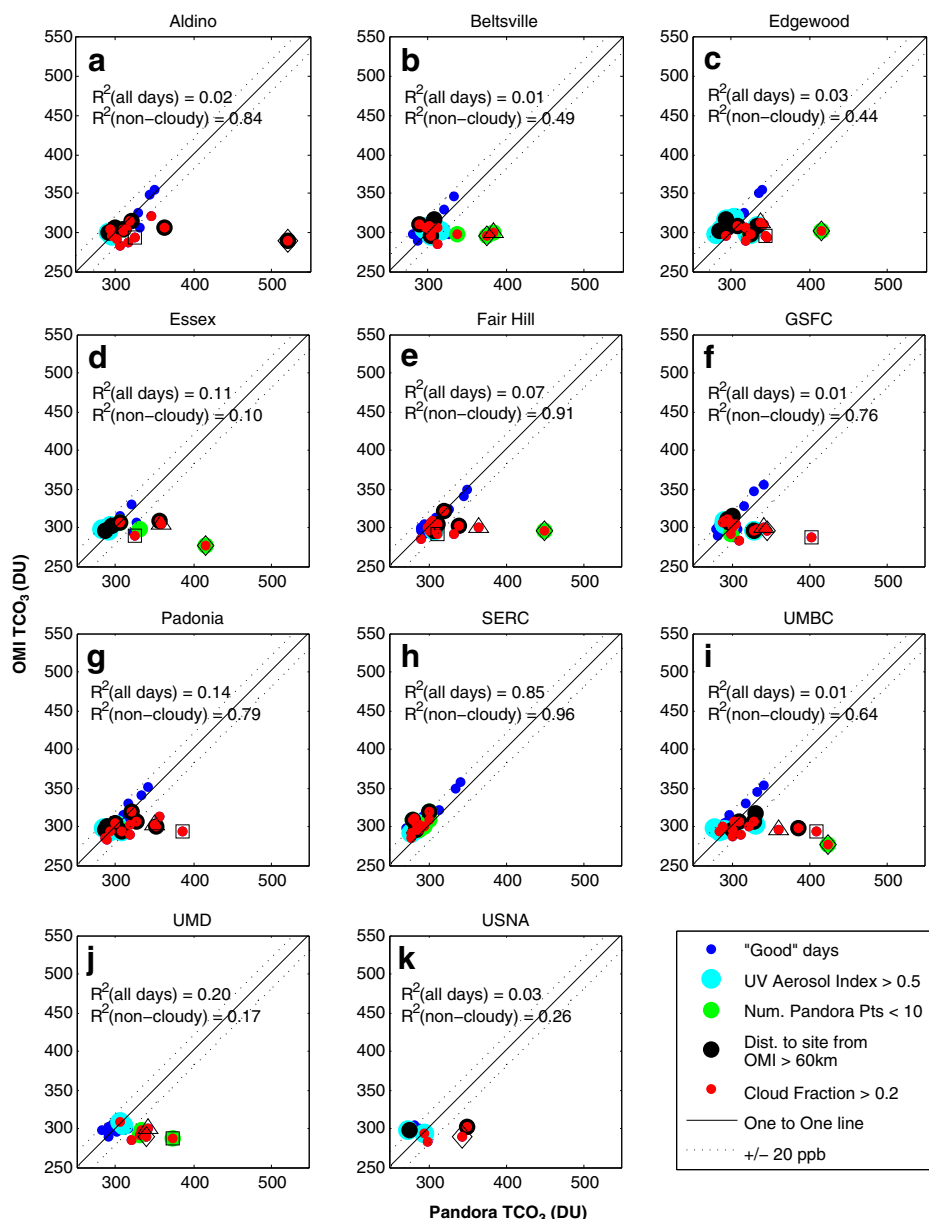


Fig. 2 OMI versus Pandora TCO₃ for July 2011 at (a) Aldino, (b) Beltsville, (c) Edgewood, (d) Essex, (e) Fairhill, (f) GSFC, (g) Padonia, (h) SERC, (i) UMBC, (j) UMD, and (k) USNA. Recurring outliers at many sites on 8 July (squares), 13 July (triangles), and 25 July (diamonds) are marked on the figure. Points are flagged for potential problems due to (red) high cloud cover, (green) number of Pandora points, (black) distance, and (cyan) UV Aerosol Index

Applying error propagation to the expected errors of OMI (1–2 %) and Pandora (1–2 %) TCO₃ retrievals given in Section 2, some days during July experienced agreement between TCO₃ retrievals from the two instruments (percent differences $\leq \sim 3\%$), whereas other days

Table 3 Daily average percent difference between Pandora and OMI TCO₃ and TCNO₂ retrievals for all available DISCOVER-AQ sites throughout July 2011

Day in July	TCO ₃	TCNO ₂				Average Cloud Fraction (from OMI) for DISCOVER-AQ sites * scattered cumulus clouds
		Average %	Number of data points contributing to average (all days)	Average %	Number of data points contributing to average (all days)	
1	2.54	15	2.54	17.79	13	17.79
2	2.65	9	2.65	23.08	9	23.08
3	2.31	15	3.89	33.17	6	—
4	4.11	7	—	70.35	3	—
5	2.91	10	3.26	—	—	0.55
6	4.00	17	1.63	40.53	9	0.21
8	13.58	17	—	26.23	2	—
9	3.46	9	3.46	24.14	9	0.68
10	3.46	18	3.19	24.59	15	24.14
11	4.15	10	4.15	25.23	9	0.05*
13	14.61	9	—	34.29	1	30.24
14	4.24	1	4.24	—	—	0.16*
15	2.71	17	2.81	34.40	13	41.41
16	—	—	—	50.22	9	0.197*
17	3.84	22	3.84	18.67	21	50.22
18	3.34	10	3.34	16.79	10	0.08*
19	7.18	15	3.87	6.67	4	17.50
20	3.77	9	3.77	19.02	9	0.13*
22	2.80	17	3.16	16.94	17	0.27
24	3.90	19	1.20	25.18	14	19.02
						0.09
						16.26
						0.25
						0.38
						14.23

Table 3 (continued)

Day in July	TCO_3	TC NO_2				Average Cloud Fraction (from OMI) for DISCOVER-AQ sites * scattered cumulus clouds
	Average %	Number of data points contributing to average (all days)	Average %	Average %	Number of data points contributing to average (all days)	Difference at all available sites (OMI—Pandora) days with cloud fraction ≤ 0.2
25	31.67	9	—	18.21	1	—
26	4.84	22	4.84	37.34	21	37.34
27	4.92	11	4.92	19.41	10	19.41
28	11.27	6	7.94	—	—	—
29	2.46	10	2.46	37.08	15	37.21
30	7.57	1	7.57	—	—	0.13*
31	2.78	18	2.81	21.62	20	22.76

during July experienced larger differences (percent differences $>\sim 3\%$), as shown in Table 3. Here, the average percent differences across all sites between both Pandora and OMI TCO_3 and Pandora and OMI TCNO_2 are provided, for both cloudy (cloud fraction >0.2) and non-cloudy (cloud fraction ≤ 0.2) days. Table 3 provides the number of comparisons contributing to each average for all days; note that discrepancies in the number of points between TCO_3 and TCNO_2 percent differences are due to different filtering techniques for the two species in the OMI overpass data. (See the AVDC and NASA GSFC website for further details.) Also included in Table 3 is the average cloud fraction from OMI data among the sites on each day at the time of the OMI overpass; days that included scattered cumulus are indicated as well. Days with scattered cumulus cloud cover are defined here as days for which the average OMI cloud fraction was less than 0.2 (non-cloudy), but for which visible images from MODIS Aqua nevertheless showed clouds in the region. Table 4 provides average percent differences by site for all days, cloudy days, and non-cloudy days.

Case studies were performed for 8, 13, and 25 July—3 days for which multiple sites in the DISCOVER-AQ campaign displayed large differences between Pandora and OMI TCO_3 retrievals (Fig. 1). We focus on results from 8 to 13 July for brevity. On these days, TCO_3 retrievals from Pandora were biased high to TCO_3 retrievals from OMI, as indicated by symbols in Fig. 2; the average percent difference was 23 %. The coordinates of points that displayed large differences on case study days are given in Table 5. The average percent difference between OMI and Pandora TCO_3 retrievals at all eleven sites on all other days during July was 4.1 %. It should also be noted that, although color coding indicates high cloud cover, distance from the center of the OMI pixel to the Pandora site, and other quality flag information (Fig. 2), no additional filtration based on this information was applied to the data used here. Large differences between the two instruments on the days mentioned above are likely the result of interference from clouds. One of the primary differences between the OMI-TOMS V8.5 algorithm and previous algorithm versions is the way in which ozone column estimation is handled in the presence of clouds. In previous versions of the retrieval algorithm, TCO_3 in the presence of clouds was determined by estimating the ozone column below cloud height (Thompson et al. 1993; Hsu et al. 1997). As a result of recent analyses that show that “the UV radiation received at the satellite is sensitive to the ozone column below the nominal cloud-top pressure”, V8.5 uses Radiative Cloud Pressure (RCP) inferred from Rotational-Raman Scattering (RRS) as the height below which the ozone column is estimated when clouds are present (Yang and Bhartia 2012). The case studies discussed here provide a validation study for this new retrieval method.

Five-minute averages from Edgewood of the absolute difference between OMI and Pandora TCO_3 retrievals, using Pandora as a reference, compared to the absolute time from the OMI overpass in five minute steps indicate that the difference between retrievals is greatest and most variable at points close in time to the OMI overpass. This phenomenon suggests that for point comparisons of OMI and Pandora TCO_3 close in time, OMI is likely missing large spatial variability (e.g., plumes, gradients due to passing fronts) in the column. Time acts as an averaging function; at larger time differences (60–120 min), the absolute differences between the two TCO_3 amounts fade out to approximately 15–20 DU. Repeating this analysis at other DISCOVER-AQ sites yielded results of the same nature; thus a 20 DU difference between the OMI and Pandora TCO_3 amounts is defined as a threshold for exceptionally poor agreement.

A comparison of OMI TCO_3 versus 1 h averages of Pandora TCO_3 (± 0.5 h window about the time of the OMI overpass) is shown in Fig. 2. High UV aerosol index values (>0.5), large distances from the center of the OMI pixel to the site (>60 km), and large cloud fractions (>0.2) are indicated on Fig. 2. Pandora averages that contain fewer than 10 retrievals are displayed too. Points outside of the ± 20 DU bounds on either side of the

Table 4 Absolute value of the average percent differences between Pandora and OMI TCO_3 and TCNO_2 at each site (Fig. 1)

Site	Absolute Value of Average % Difference for July TCO_3			Absolute Value of Average % Difference for July TCNO_2		
	All Days	Cloudy Days (Cloud Fraction >0.2)	Non-cloudy Days (Cloud Fraction ≤ 0.2)	All Days	Cloudy Days (Cloud Fraction >0.2)	Non-cloudy Days (Cloud Fraction ≤ 0.2)
Edgewood	6.40	10.40	4.81	32.91	72.04	28.99
Aldino	4.74	9.76	1.81	25.83	41.85	21.61
Beltsville	4.87	8.08	3.19	28.10	27.79	28.20
Essex	7.24	16.72	3.94	29.04	21.58	29.62
Fair Hill	3.88	8.55	1.84	26.95	21.17	28.53
GSFC	5.88	8.96	4.06	29.57	24.21	31.72
Padonia	5.04	7.74	3.44	25.25	38.50	22.10
SERC	2.50	1.91	2.85	15.59	14.16	16.12
UMBC	7.41	11.53	4.39	24.06	23.80	24.20
UMD	6.07	13.12	2.54	44.21	51.86	42.30
USNA	7.84	9.22	7.15	13.82	10.66	14.87

Table 5 Pandora (P) and OMI (O) values at sites with poor agreement on case study days

Site	TCO ₃						TCNO ₂					
	8 July			13 July			25 July			6 July		
	P	O	P	O	P	O	P	O	P	O	P	O
Aldino	324.6	293.6	—	—	522.5	289.0	3.9E15	7.6E15	—	—	5.5E15	7.9E15
Bethsville	—	—	384.6	299.0	374.8	295.4	1.2E16	5.6E15	1.5E16	6.6E15	1.0E16	4.5E15
Edgewood	345.9	294.0	338.1	313.3	415.1	301.8	1.2E16	6.9E15	1.4E16	7.9E15	—	1.3E16
Essex	324.6	289.0	358.7	304.2	416.7	275.8	—	—	—	6.7E15	3.4E15	—
Fair Hill	332.0	291.4	365.0	299.0	449.9	296.0	—	—	—	—	4.6E15	7.0E15
GSFC	404.0	287.8	341.1	299.0	345.9	295.4	7.1E15	5.2E15	1.1E16	5.9E15	6.6E15	4.5E15
Padonia	386.9	293.6	350.6	301.7	—	—	—	—	—	—	8.4E15	1.2E16 2.0E16
SERC	—	—	—	—	—	—	—	—	7.0E15	4.3E15	—	—
UMBC	408.6	292.7	360.4	296.4	424.3	275.8	—	—	—	9.2E15	4.0E15	9.9E15
UMD	373.6	287.8	341.0	299.0	338.6	289.9	1.1E16	5.2E15	1.5E16	5.9E15	9.8E15	4.5E15
USNA	—	—	—	—	342.7	290.0	—	—	—	6.0E15	4.3E15	—

one-to-one line are designated as having large differences between OMI and Pandora TCO₃ retrievals. There are several noteworthy features in Fig. 2. First, on days for which OMI indicates a cloud fraction >0.2, Pandora tends to retrieve a higher TCO₃ amount than OMI. This is expected, due to multiple scattering increasing the effective air mass factor (AMF), and also due to uncertainties in OMI estimates of ozone amounts below the cloud.

With the exception of a few days with high cloud fractions, the Aldino, Fairhill, and Smithsonian Environmental Research Center (SERC) sites exhibit good correlation between OMI and Pandora TCO₃ retrievals (Fig. 2). The consistency between Pandora and OMI TCO₃ retrievals at these sites may be attributed to their respective locations relative to the major urban areas of Baltimore and Washington, D.C. The relatively coarse resolution of OMI (13×24 km at nadir) can lead to averaging of pollutants in adjacent rural and urban locations, which can cause large differences between ground- and satellite-based total column retrievals. Fairhill and Aldino are 101 km and 54 km northeast of Baltimore, respectively. Fairhill is the most rural site in the campaign. Though SERC is only about 42 km from Washington, D.C., it is in a rural and wooded area along the Chesapeake Bay containing 10.7 km² of forest.

Figure 3 provides an overview of clouds and moisture in the atmosphere in the DISCOVER-AQ region on 8 July 2011. The visible image from MODIS Aqua (Fig. 3a) on 8 July 2011 indicates that there was heavy cloud cover in the region at the time of the OMI overpass; the visible image from 13 July (not shown) suggests similar cloud cover. As indicated in Fig. 2, sites with large differences on these two dates had a cloud fraction >0.2; the visible images (Fig. 3a) show the vast coverage of clouds (cloud fraction as high as 0.9) in the region at the time of the overpass. Because of the extensive cloud cover in the region on these 2 days (Table 3, Fig. 3a), other possible error sources were ruled out as being potentially significant.

Information provided by the MERRA Model output furthers our insight into the cloud cover on 8 July 2011. Cloud liquid water mixing ratio from MERRA on 8 July (Fig. 3b) shows that there were significant levels of moisture throughout the atmosphere. Cloud-top pressure from the MERRA Model on 8 July (Fig. 3c) shows that clouds were distributed at varying levels throughout the atmosphere, with cloud-top heights ranging from approximately 200 hPa to 1,000 hPa. An analysis of cloud cover on 13 July 2011 revealed similar results. Varying cloud-top heights may cause inaccurate TCO₃ retrievals, particularly for OMI. Given that OMI must estimate O₃ levels below clouds, if cloud top heights within a pixel are not uniform, estimates of O₃ become more prone to error.

The extensive cloud cover over the DISCOVER-AQ region on 8 and 13 July had adverse affects on OMI and Pandora TCO₃ retrieval comparisons, agreeing with Tzortziou et al. (2012). On days with extensive cloud cover (>0.2), OMI consistently shows lower TCO₃ values compared to the Pandora retrievals.

Using data from the Edgewood, Maryland site, it is seen that the unusual rises in Pandora TCO₃ on days with high cloud cover correspond to a sharp drop in j_{NO2}. This quantity is proportional to actinic flux and the number of UV photons in the atmosphere. As the amount of UV radiation in the atmosphere on 8 July drops due to cloud cover, Pandora TCO₃ retrievals become unusually high, rising to near 500 DU (Fig. 4). The high TCO₃ retrievals from Pandora in these cases are apparent artifacts. As expected, the diminished UV radiation during these time periods prevents Pandora, a direct sun spectrometer, from retrieving accurate TCO₃ levels. Figure 4c illustrates typical j_{NO2} time series during the afternoon hours for days with clear skies, days with scattered cumulus clouds, and days with cloudy skies. Uncertainties in OMI retrievals under cloudy conditions, due to uncertainties in the estimates of ozone amounts below the cloud are also responsible for the large inconsistencies between the two sensors on the days with extensive (cloud fraction >0.2) cloud cover.

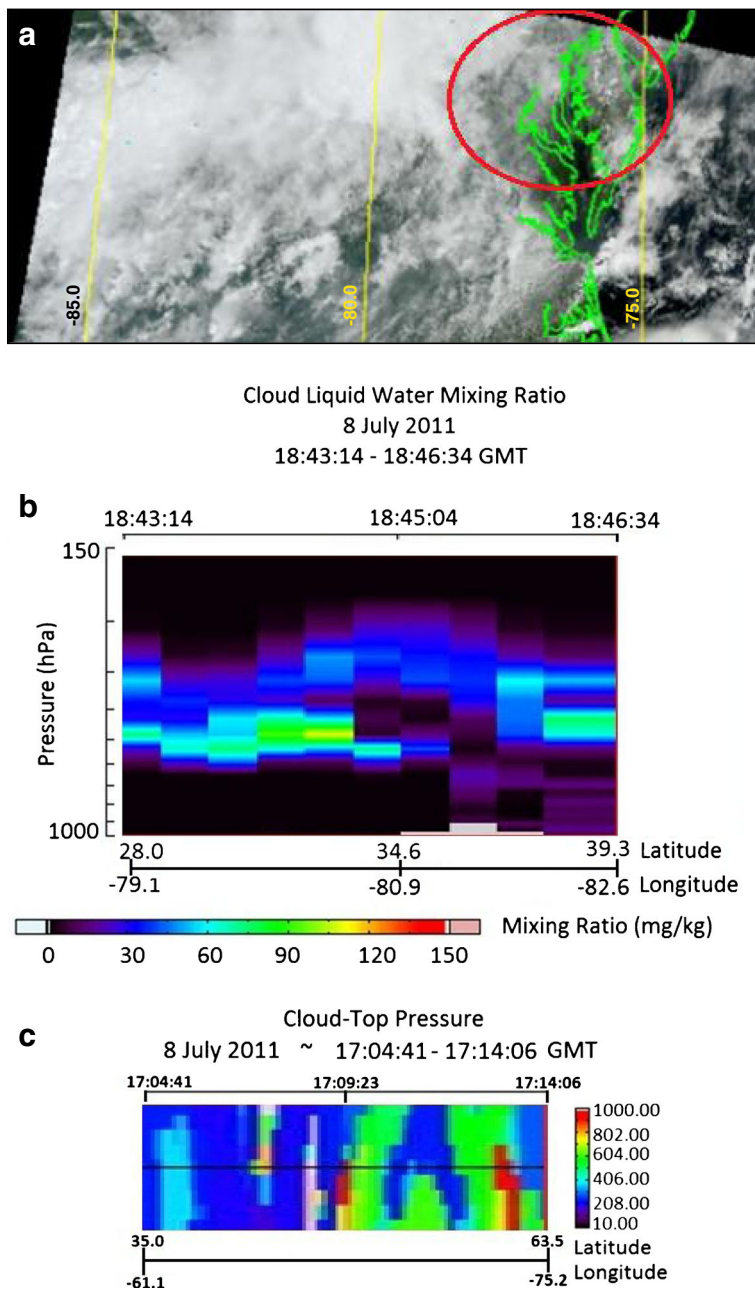


Fig. 3 (a) Visible satellite image from MODIS Aqua showing cloud cover over the DISCOVER-AQ region (red circle) on 8 July 2011 near the time of the OMI overpass. (b) MERRA Model outputs of cloud liquid water mixing ratio in the region on 8 July 2011. (c) MERRA Model output showing the cloud-top pressure in the region on 8 July 2011

We also use ozonesondes as a reference to compare with both Pandora and OMI TCO₃ at Edgewood and Beltsville, Maryland. Figure 5a compares TCO₃ from the Edgewood OMI

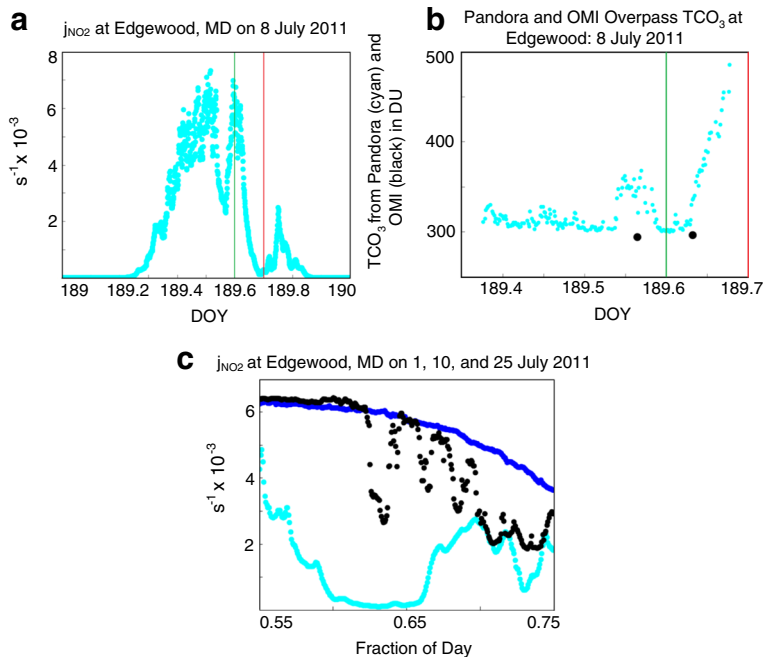


Fig. 4 (a) j_{NO_2} and (b) TCO₃ retrievals from OMI (black) and Pandora (cyan) at Edgewood, Maryland, on 8 July 2011. Green and red lines on plots (a) and (b) represent the same starting and ending times, respectively. DOY is given in local time. (c) j_{NO_2} at Edgewood on 1 July (clear; blue), 10 July (scattered cumulus; black), and 25 July (cloudy; cyan). Fraction of day is given in local time

overpass to TCO₃ from the July 2011 Edgewood ozonesondes. Better agreement exists between OMI and the ozonesonde TCO₃ than between Pandora and the ozonesonde TCO₃ (Fig. 5b). Pandora data points (Fig. 5b) are one-hour averages of TCO₃ retrievals centered on the midpoint of the ozonesonde flight time. The apparent artifact in the Pandora data caused by cloudy conditions is evident in the comparison of Pandora and ozonesonde TCO₃. Ozonesondes in this

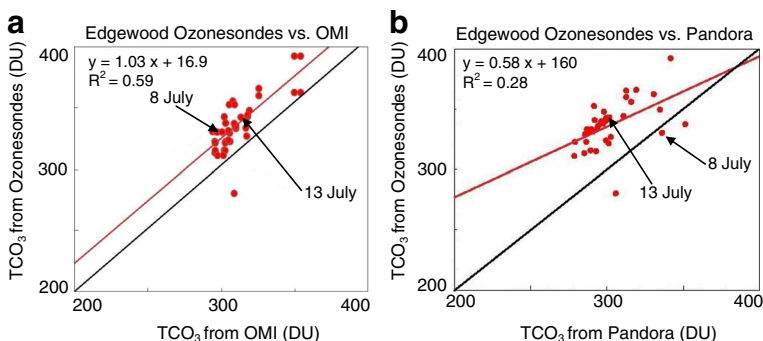


Fig. 5 (a) OMI TCO₃ versus ozonesonde TCO₃ at Edgewood, Maryland, during July 2011. (b) Pandora TCO₃ versus ozonesonde TCO₃ at Edgewood, Maryland, during July 2011. Black one-to-one lines and red best-fit lines, as well as the equations of the best-fit lines are included. Comparisons to profiles on the 8 and 13 of July are indicated; there was no profile on 25 July

campaign were generally biased to higher TCO_3 values than Pandora, OMI, or other satellite products (Martins et al. *this issue*; Thompson et al. *this issue*); cases for which the Pandora and ozonesonde column abundances are in a nearly 1:1 ratio tend to correspond to cloudy days that result in an artifact in the Pandora data. Additionally, outlier points in the comparison of Pandora and ozonesonde column abundances for which the Pandora column is lower than the ozonesonde column tend to occur on clear days when Pandora data is not affected by the cloud-induced artifact. Correlation between OMI and ozonesonde TCO_3 is somewhat better than that between Pandora and ozonesonde TCO_3 ; however, there is almost a 17 DU bias between OMI and ozonesonde TCO_3 . The outlier point for which OMI TCO_3 is greater than ozonesonde TCO_3 occurs on 28 July; it is probable that cloud cover on this day adversely affected the OMI TCO_3 retrieval (Table 3). Although there were fewer profiles, and the results are not shown here, Beltsville ozonesondes compared similarly to Pandora and OMI data.

4 TCNO_2

Some days during July show good agreement between TCNO_2 retrievals from Pandora and OMI at many sites (percent difference $\leq 30\text{--}60\%$), whereas other days during July show percent differences between the two instruments at some sites that are larger than 60 % (Table 3). Table 4 shows the monthly average of percent differences between TCNO_2 retrievals at each site. Percent differences in Tables 3 and 4 are calculated for both cloudy (cloud fraction >0.2) and non-cloudy conditions. Note that in all other instances, no filtration for cloud cover, aerosols, or distance from the center of the OMI pixel to the Pandora site was applied to the TCNO_2 data used here.

At Edgewood, five-minute averages of the absolute difference between OMI and Pandora TCNO_2 retrievals, $|OMI_{\text{TCNO}_2} - Pandora_{\text{TCNO}_2}|$, were compared to the absolute time from the OMI overpass in 5 min steps. Similar to the comparison made for TCO_3 , time acts as an averaging function, causing the absolute differences between the two TCNO_2 amounts fade out to approximately 0.06 DU, or $\sim 1.6 \times 10^{15}$ molecules/cm² at greater (1–2 h) time differences. Repeating this analysis at other DISCOVER-AQ sites yielded similar results; thus a 1.6×10^{15} molecules/cm² difference between the OMI and Pandora TCNO_2 amounts is defined as a threshold for large differences between the two instrument retrievals.

Figure 6 shows a comparison of OMI TCNO_2 and 1-hour averages of Pandora TCNO_2 centered on the time of the OMI overpass. Retrievals that are from pixels on the ends of the OMI swath, large distances (>60 km) from the center of the OMI pixel to the site, or contaminated by large cloud fractions (>0.2) are indicated on Fig. 6. Pandora averages that contain less than one-third of the expected retrievals (<10) in an hour are also shown. Additionally, points that saw poor agreement on case study days are indicated by symbols in Fig. 6; the coordinates of these points are given in Table 5. Points outside of the $\pm 1.6 \times 10^{15}$ molecules/cm² bounds on either side of the one-to-one line are considered to exhibit poor agreement between OMI and Pandora TCNO_2 retrievals.

Many of the comparisons shown in Fig. 6 indicate that the OMI overpass pixel was very close to the edge of the swath. These pixels have a resolution that is not as fine as those at nadir; thus, less accurate TCNO_2 retrievals may result, due to more averaging of pollutants within the larger pixel. The agreement between Pandora and OMI TCNO_2 is generally worse than the agreement between Pandora and OMI TCO_3 (Figs. 2 and 6).

As with the TCO_3 retrieval comparisons, SERC shows some of the best correlation between Pandora and OMI TCNO_2 (Fig. 6). As discussed previously, this could be due to smaller atmospheric variability in the rural environment in which SERC is located.

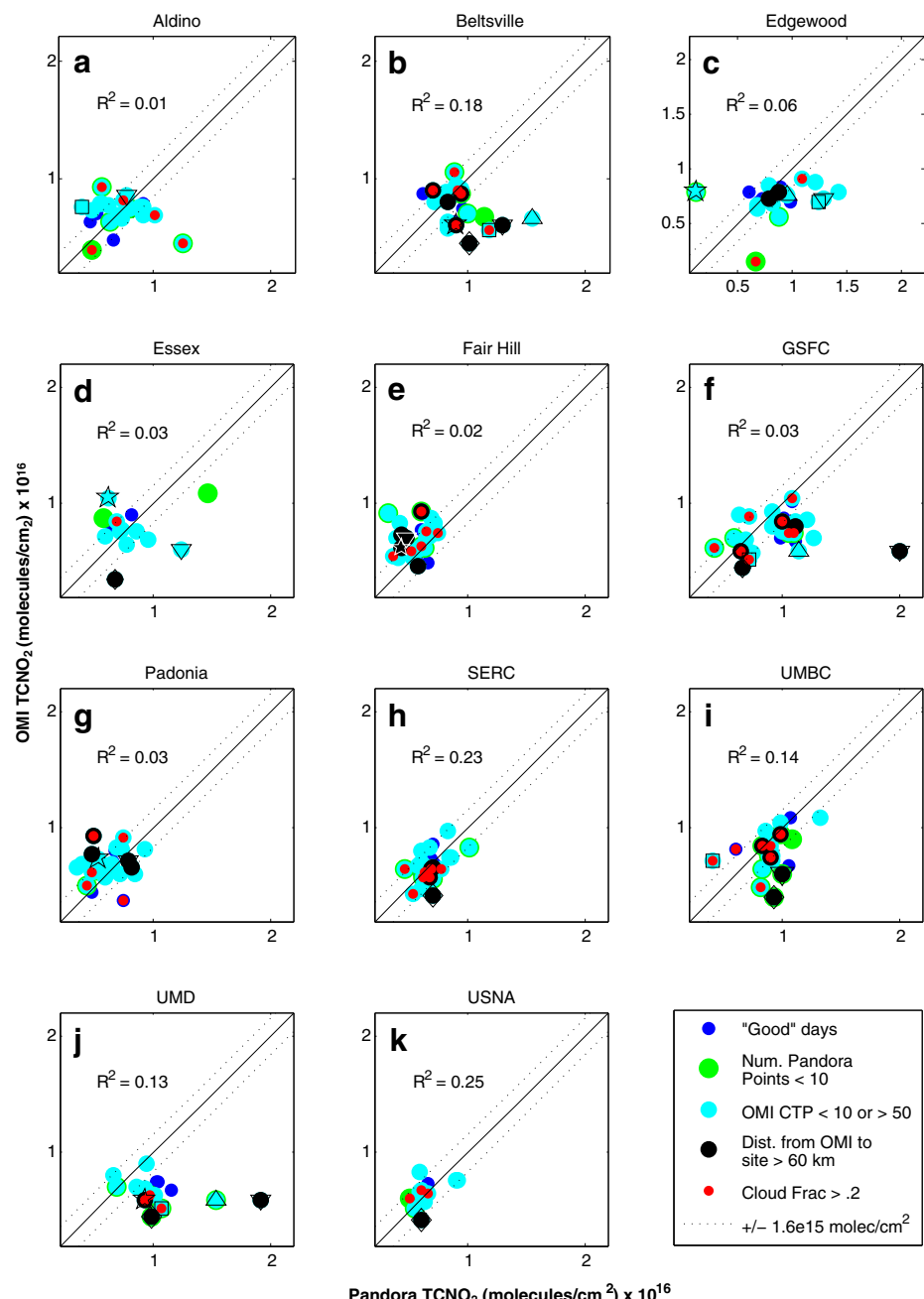


Fig. 6 OMI versus Pandora TCNO₂ for July 2011 at (a) Edgewood, (b) Aldino, (c) Beltsville, (d) Essex, (e) Fairhill, (f) GSFC, (g) Padonia, (h) SERC, (i) UMBC, (j) UMD, and (k) USNA. 6 July (squares), 15 July (upward triangles), 16 July (diamonds), 26 July (downward triangles), and 29 July (stars) were recurring outliers at many sites, and are marked on the figure. Points are flagged for high cloud cover (red), number of Pandora points (green), distance (black), and OMI CTP (cyan)

However, the United States Naval Academy (USNA) in Annapolis is a site with relatively good agreement between Pandora and OMI TCNO₂ compared to other sites in the campaign as well (Fig. 6). Though there are not as many retrievals available for comparison at USNA as at SERC, it is interesting that these two sites, within close proximity to one another, display some of the best agreement between TCNO₂ retrievals. Additional observations of this region are necessary to be conclusive about the agreement between OMI and Pandora TCNO₂ retrievals.

The comparisons that are illustrated in Fig. 6 indicate that on some specific days, multiple sites exhibit large differences between the TCNO₂ retrievals from OMI and Pandora (e.g. 6 July (DOY 187), 15 July (DOY 196), 16 July (DOY 197), 26 July (DOY 207), and 29 July (DOY 210)). The average percent difference between OMI and Pandora retrievals in these cases was 65 %, while the average percent difference between retrievals at the eleven sites on all other days during July 2011 was 25 %. Case studies were performed for the DISCOVER-AQ region on these days to determine the cause of the large differences between TCNO₂ retrievals; for brevity, the results are reported for 15, 16, and 26 July 2011.

4.1 Case studies: 15 and 16 July 2011

Figure 6 illustrates that Beltsville, Edgewood, GSFC, and UMD all showed large differences between Pandora and OMI TCNO₂ retrievals on 15 July 2011. Beltsville, Essex, GSFC, SERC, UMBC, UMD, and USNA all exhibited large differences between Pandora and OMI TCNO₂ retrievals on 16 July 2011.

An overview of clouds and moisture in the atmosphere over the DISCOVER-AQ region on 15 July 2011 is provided in Fig. 7. The visible image from MODIS Aqua (Fig. 7a) presents primarily small, scattered clouds in the region during the OMI overpass on 15 July 2011. These clouds, typical of fair weather on a summer day, can block the field of view for Pandora, but are not usually substantial enough to cause OMI to register a high (>0.2) cloud fraction (Table 3). The scattering of light by these clouds can cause retrieval errors for both instruments. MODIS Aqua images revealed similar cloud cover on 16 July 2011. In addition to information obtained from MODIS, cloud liquid water mixing ratio from MERRA model output shows that there were significant levels of moisture throughout the atmosphere on July 15, and that cloud-top pressures ranged between 100 hPa and 700 hPa, an indication of the varied cloud cover in the region. This general pattern of scattered clouds at varying heights prevailed on 16 July 2011 as well (Table 3).

In addition to cloud cover, local chemistry and transport on 15 and 16 July are considered. Note that the majority of NO₂ in a column is located within the boundary layer. On 15 July 2011, 24-hour back trajectories indicate that winds were from regions with TCNO₂ amounts slightly lower than those retrieved in the DISCOVER-AQ area. This transport could have contributed to the differences between Pandora and OMI TCNO₂ retrievals. Local chemistry and transport were similar on 16 July 2011.

The presence of aerosols in the DISCOVER-AQ region on 15 and 16 July 2011 was also considered when determining why these days were outliers in TCNO₂ retrieval comparisons. According to both the MODIS Aqua image in Fig. 8, and the CIMEL photometer at GSFC, there was some low-level light extinction in the atmosphere on 15 July 2011, with AOD at 550 nm between 0.18 and 0.26 according to MODIS, and an AOD value of 0.23 according to the CIMEL. AOD from MODIS Aqua was 0.02–0.18 on 16 July 2011. The UV Aerosol Index from OMI on 15 July 2011 indicated that amounts of UV-absorbing aerosols present in the atmosphere at this time were insignificant. These data were not available for 16 July

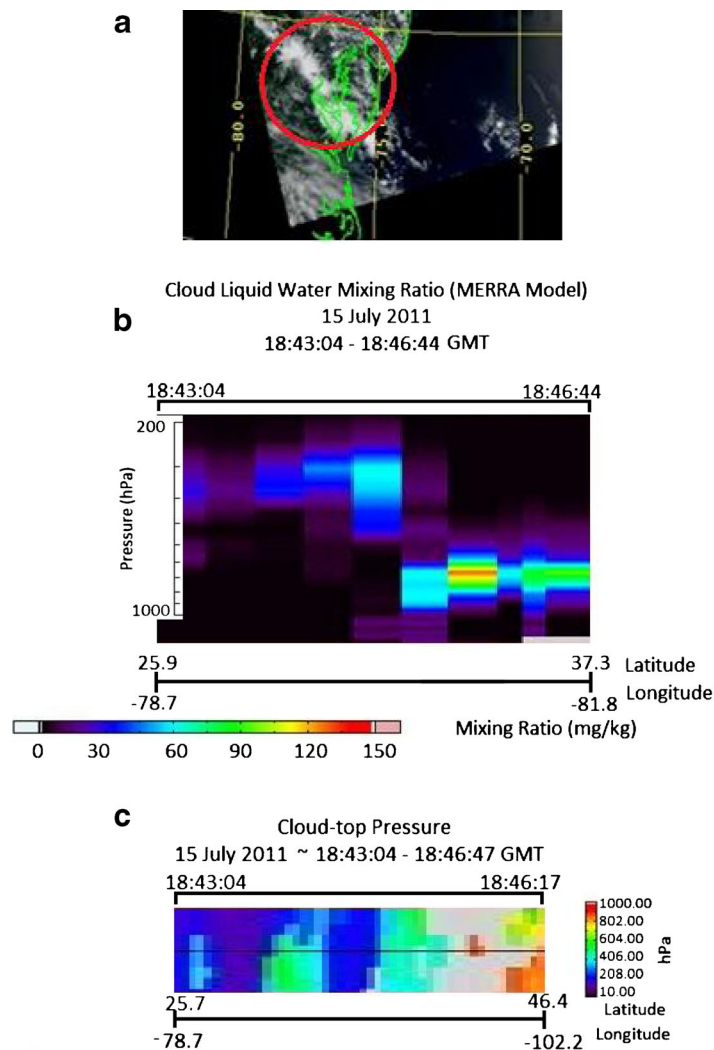
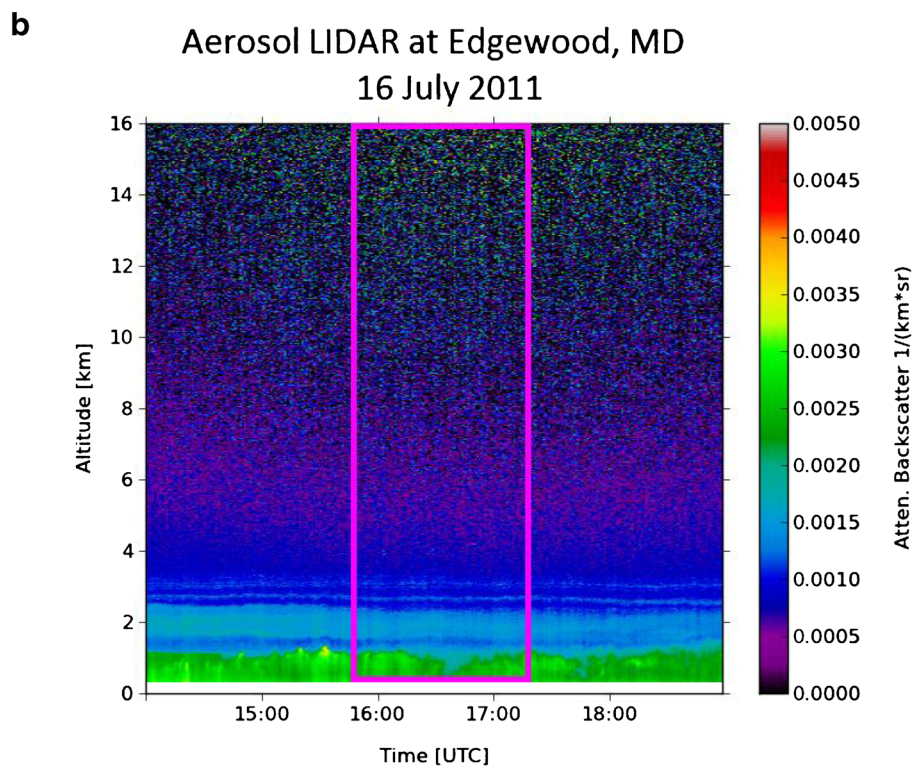
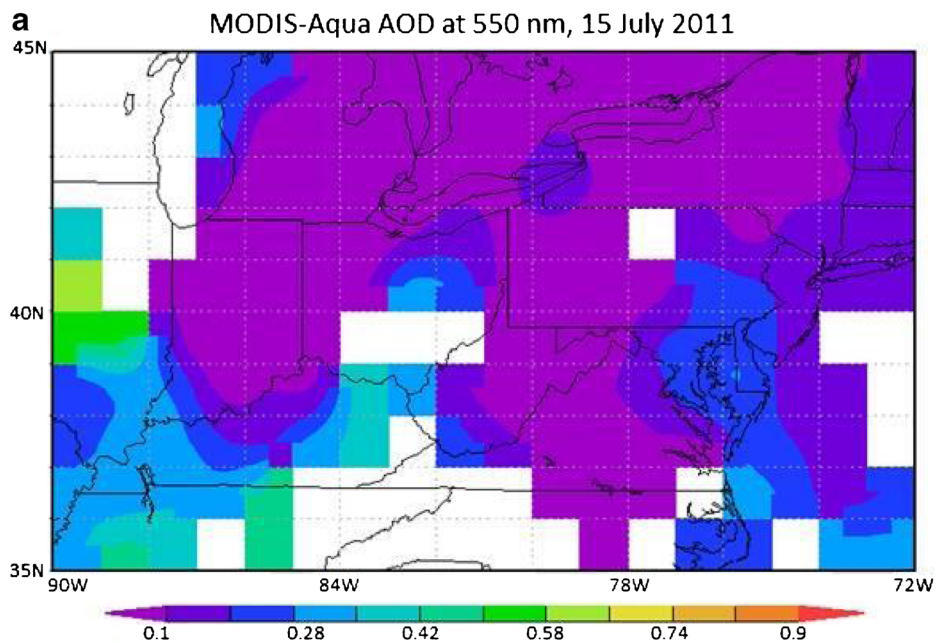


Fig. 7 (a) Visible satellite image from MODIS Aqua showing cloud cover over the DISCOVER-AQ region (red circle) on 15 July 2011 near the time of the OMI overpass. (b) MERRA Model output of cloud liquid water mixing ratio in the region on 15 July 2011. (c) MERRA Model output showing the cloud-top pressure in the region on 15 July 2011

2011. Finally, the aerosol LIDAR shown in Fig. 8b from 16 July 2011 is representative of LIDAR images for both days. Some backscatter is indicated low in the atmosphere during the time of the OMI overpass; however, it is unlikely that this backscatter caused large errors for OMI or Pandora retrievals.

Figure 8 suggests that aerosols were not a major factor contributing to large differences between TCNO_2 retrievals from Pandora and OMI on 15 or 16 July 2011. These results also suggest that scattered, passing cumulus clouds in the DISCOVER-AQ region on 15 and 16 July were the major source of the large differences between OMI and Pandora TCNO_2



◀ **Fig. 8** (a) Aerosol Optical Depth (unitless) at 550 nm from MODIS Aqua on 15 July 2011. Latitude (degrees) is given on the y-axis; longitude (degrees) is given on the x-axis. (b) Backscattering measurements (units of attenuated backscatter) from the Micropulse Lidar instrument at Edgewood, Maryland on 16 July 2011. The purple box indicates the approximate time period of the OMI overpass

retrievals, a conclusion that has not been indicated in previous studies comparing TCNO₂ from the two instruments. Moving clouds can cause saturation to occur during the 20-second measurement window used to retrieve NO₂. If this occurs, Pandora data are not saved. The passing cumulus clouds could have resulted in fewer Pandora retrievals available to average for comparison with the OMI TCNO₂ retrieval. This type of scattered cloud cover does not cause OMI to indicate a high cloud fraction. However, such cloud cover may result in erroneous retrievals from either Pandora or OMI due to scattered radiation from the clouds (Fig. 4c; Boersma et al. 2002).

Comparisons were also made between Pandora TCNO₂ retrievals at Edgewood, Maryland and ground measurements of surface NO₂ concentrations (in ppbv) from the Teledyne API EU NO_x Analyzer at the same site. Although the two instruments do not measure the same quantity, the diurnal pattern of TCNO₂ measured by Pandora was consistent with diurnal variability in surface NO₂ on 10 July 2011, with both instruments indicating a plume around mid-day (Knepf et al. 2012). Similar agreement in diurnal patterns observed by the two instruments was typical for 15 and 16 July 2011 as well.

4.2 Case study: 26 July 2011

Unlike our previous case studies, 26 July had mainly clear skies in the DISCOVER-AQ region. Agreement between Pandora and OMI TCNO₂ retrievals was nevertheless poor at multiple sites (Fig. 6). Aldino, Beltsville, Edgewood, Essex, Fairhill, GSFC, Padonia, UMBC, and UMD all had large differences between Pandora and OMI TCNO₂ retrievals on this day.

An overview of the clouds and moisture in the atmosphere in the DISCOVER-AQ region on 26 July 2011 is provided in Fig. 9. The visible image from MODIS Aqua (Fig. 9a) shows that skies in the area during the OMI overpass were mainly clear. This assessment agrees well with Fig. 6, in which none of the sites were flagged as having a high cloud fraction on 26 July. MERRA model cloud liquid water mixing ratio from about an hour after the OMI overpass indicates that some clouds may have entered the region afterwards (Fig. 9b). OMI Level 3 TCNO₂ retrievals in and surrounding the DISCOVER-AQ region, and HYSPLIT back trajectories from the region (not shown), suggest that local chemistry and transport were not major causes of the large differences between OMI and Pandora TCNO₂ retrievals on 26 July 2011, either.

According to the relatively low AODs from MODIS (between approximately 0.02 and 0.1) and CIMEL (approximately 0.085), there was minimal light extinction due to scattering or absorption throughout most of the atmosphere on this date (Fig. 10). UV Aerosol Index from OMI indicated that there were not significant levels of UV-absorbing aerosols present in the DISCOVER-AQ region on 26 July 2011. The aerosol LIDAR aboard NATIVE measured moderate levels of backscatter in the atmosphere during the time of the OMI overpass (Fig. 10b). A second aerosol LIDAR also located in Edgewood, however, measured a great deal of backscatter in the boundary layer during the approximate time of the OMI overpass on this day (Fig. 10c). Given the clear skies shown in Fig. 9a, and the lower backscatter indicated in the AOD values and the NATIVE LIDAR, the backscatter in

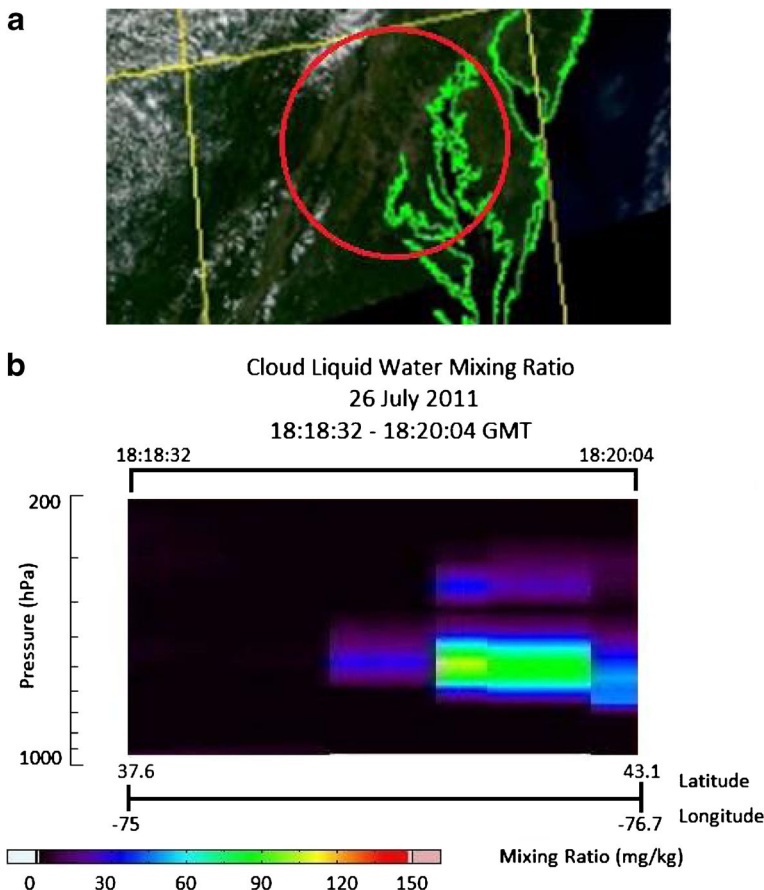
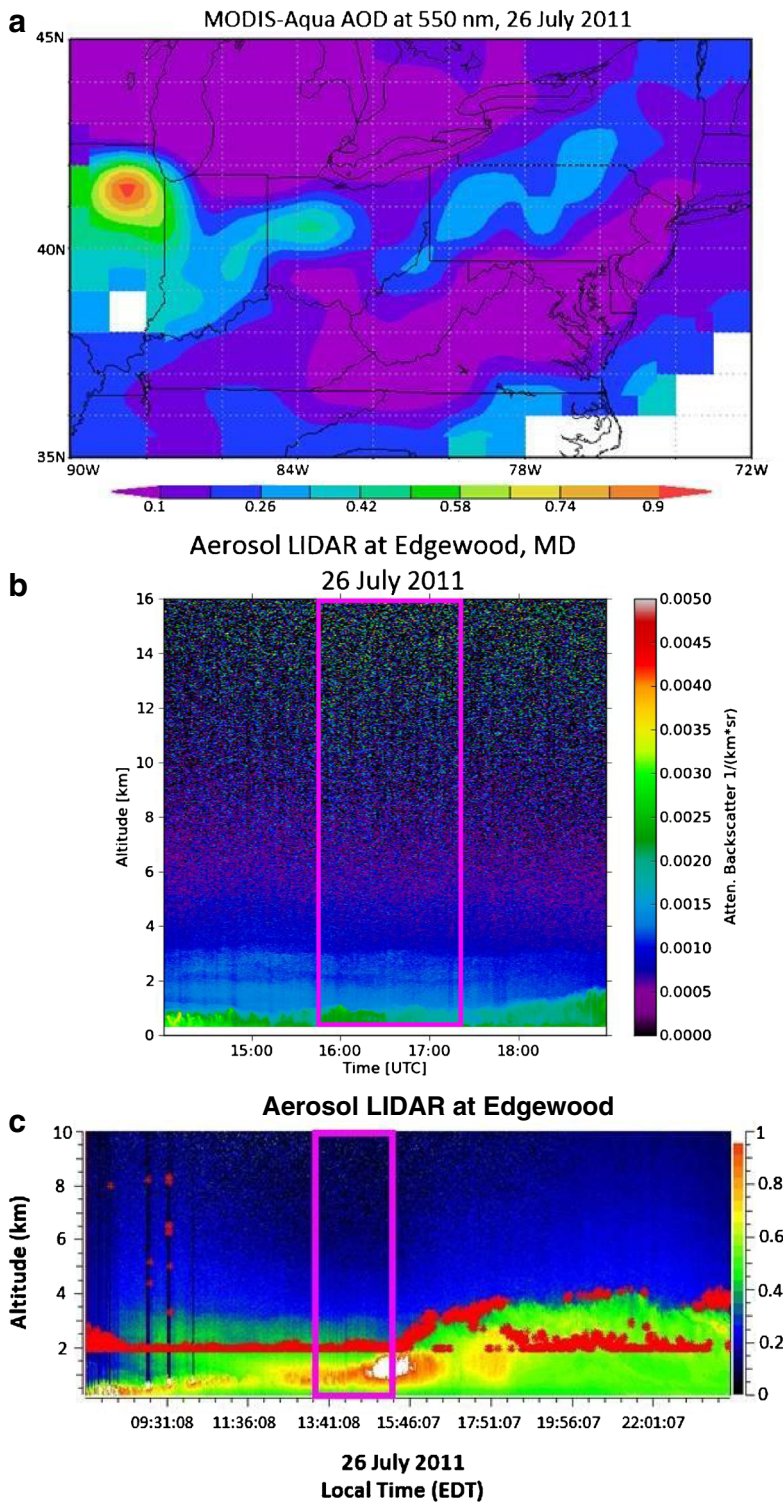


Fig. 9 (a) Visible satellite image from MODIS Aqua showing cloud cover over the DISCOVER-AQ region (red circle) on 26 July 2011 near the time of the OMI overpass. (b) MERRA Model output of cloud liquid water mixing ratio in the region on 26 July 2011

Fig. 10c may be caused by a low-altitude plume of scattering aerosols. Scattering aerosol plumes in regions of the boundary layer are likely a significant influence on the comparison between OMI and Pandora TCNO₂ retrievals on 26 July. Case studies similar to those described above indicate that the cause of large differences between OMI and Pandora TCNO₂ retrievals on 6 and 29 July 2011 was a combination of scattered cloud cover and aerosols.

Fig. 10 (a) Aerosol Optical Depth (unitless) at 550 nm from MODIS Aqua on 26 July 2011. Latitude ► (degrees) is given on the y-axis; longitude (degrees) is given on the x-axis. (b) Backscattering measurements (units of attenuated backscatter) from the Micropulse Lidar instrument at Edgewood, Maryland on NATIVE on 26 July 2011. Time is in local time. The purple box indicates the approximate time period of the OMI overpass. (c) Backscattering measurements (unitless) from the Micropulse Lidar instrument at Edgewood, Maryland, operated by the Millersville University research group, on 26 July 2011. Time is in local time. The purple box indicates the approximate time period of the OMI overpass



5 Conclusions

A study of Pandora and OMI TCO_3 and TCNO_2 retrievals from the Washington, D.C., and Baltimore, Maryland, metropolitan area during the NASA-sponsored July 2011 DISCOVER-AQ campaign revealed overall good agreement between the two instruments, consistent with previous studies (Herman et al. 2009; Tzortziou et al. 2012). Residuals were within $\pm 4.5\%$ for TCO_3 , and within $\pm 25\%$ for TCNO_2 .

Consistent with Tzortziou et al. (2012), TCO_3 retrievals for the two instruments generally agree well on days for which the cloud fraction at the time of the OMI overpass is ≤ 0.2 (Fig. 2, Table 3). Additionally, TCO_3 retrievals from OMI and Pandora exhibit better agreement at rural locations, such as Fair Hill, Maryland, than at the more urban sampling sites in the 2011 DISCOVER-AQ campaign. Retrievals of TCNO_2 from Pandora and OMI at the locations of SERC and USNA exhibited the best agreement among sites included in this study (Figs. 2 and 6). This could be due to lower atmospheric variability expected in the rural region in which both instruments were located.

Measurements of surface NO_2 from the Teledyne API 200 EU NO_x Analyzer at Edgewood, MD were in good agreement with the TCNO_2 diurnal patterns measured by Pandora, suggesting that most of the observed variability in NO_2 was within the boundary layer. As expected, substantially cloudy conditions (cloud fraction > 0.2) on certain days during the campaign caused retrieval errors for TCO_3 , resulting in an average percent difference of 23 % between retrievals. In contrast, scattered cloud cover that does not result in a high (> 0.2) cloud fraction, and aerosol layers, were the main factors adversely affecting TCNO_2 comparisons, with an average percent difference of 65 % between NO_2 retrievals in such conditions. Because different environmental factors affect the TCO_3 and TCNO_2 retrievals, days that show large differences between TCO_3 retrievals are not the same as days that show large differences between TCNO_2 retrievals.

Acknowledgments This work was supported by a National Aeronautics and Space Administration (NASA) DISCOVER-AQ grant (NNX10AR39G), with additional support from NNX08AJ15G and NNX10AQ11A. The authors would like to thank the co-PIs of DISCOVER-AQ James Crawford (NASA-LARC) and Kenneth Pickering (NASA-GSFC), as well as the members of the Gator Research team (PSU) for their support and contributions.

Open Access This article is distributed under the terms of the Creative Commons Attribution License which permits any use, distribution, and reproduction in any medium, provided the original author(s) and the source are credited.

References

- Anton, M., Lopez, M., Vilaplana, J.M., Kroon, M., McPeters, R., Banon, M., Serrano, A.: Validation of OMI-TOMS and OMI-DOAS total ozone column using five Brewer spectroradiometers at the Iberian peninsula. *J. Geophys. Res.* **114**, D14307 (2009). doi:[10.1029/2009JD012003](https://doi.org/10.1029/2009JD012003)
- Berkoff, T.A., Welton, E.J., Campbell, J.R., Scott, V.S., Spinhirne, J.D.: Investigation of Overlap Correction Techniques for the Micro-Pulse Lidar NETwork (MPLNET), Geoscience and Remote Sensing Symposium, 2003. IGARSS'03. Proceedings. 2003 IEEE International **7**, 4395–4397 (2003). doi:[10.1109/IGARSS.2003.1295527](https://doi.org/10.1109/IGARSS.2003.1295527)
- Bhartia, P. K., Wellemeyer, C. W.: OMI TOMS-V8 Total O₃ algorithm, algorithm theoretical baseline document: OMI ozone products. P. K. Bhartia (ed.), vol. II, ATBD-OMI-02, version 2.0 (2002)
- Boersma, K. F., Bucsela, E., Brinksma, E., Gleason, J. F.: NO₂, Algorithm theoretical baseline document: OMI trace gas algorithms. K. Chance (ed.), vol. IV, ATBD-OMI-04, version 2.0 (2002)

Boersma, K. F., Jacob, D. J., Bucsela, E. J., Perring, A. E., Dirksen, R., van der A, R. J., Yantosca, R. M., Park, R. J., Wenig, M. O., Bertram, T. H., Cohen, R. C.: Validation of OMI tropospheric NO₂ observations during INTEX-B and application to constrain NOx emissions over the Eastern United States and Mexico, *Atmospheric Environment*, **42** (2008)

Bosilovich, M. G.: NASA's modern era retrospective-analysis for research and applications: Integrating earth observations. <http://www.earthzine.org/2008/09/26/nasas-modern-era-retrospective-analysis> (2008)

Brinksma, E.J., Pinardi, G., Volten, H., Braak, R., Richter, A., Schonhardt, A., van Roozendael, M., Fayt, C., Hermans, C., Dirksen, R.J., Vlemmix, T., Berkhouit, A.J.C., Swart, D.P.J., Oetjen, H., Wittrock, F., Wagner, T., Ibrahim, O.W., de Leeuw, G., Moerman, M., Curier, R.L., Celarier, E.A., Cede, A., Knap, W.H., Veefkind, J.P., Eskes, H.J., Allaart, M., Rothe, R., Piters, A.J.M., Levelt, P.F.: The 2005 and 2006 DANDELIONS NO₂ and aerosol intercomparison campaigns. *J. Geophys. Res.* **113**, D16S46 (2008). doi:[10.1029/2007JD008808](https://doi.org/10.1029/2007JD008808)

Bucsela, E. J., Celarier, E. A., Wenig, M. O., Gleason, J. F., Veefkind, J. P., Folkert Boersma, K., Brinksma, E. J.: Algorithm for NO₂ vertical column retrieval from the ozone monitoring instrument, *IEEE Transactions on Geoscience and remote sensing*, **44** (2006). doi: [10.1109/TGRS.2005.863715](https://doi.org/10.1109/TGRS.2005.863715)

Bucsela, E.J., Perring, A.E., Cohen, R.C., Boersma, K.F., Celarier, E.A., Gleason, J.F., Wenig, M.O., Bertram, T.H., Wooldridge, P.J., Dirksen, R., Veefkind, J.P.: Comparison of tropospheric NO₂ from in situ aircraft measurements with near-real-time and standard product data from OMI. *J. Geophys. Res.* **113** (2008). doi:[10.1029/2007JD008838](https://doi.org/10.1029/2007JD008838)

Celarier, E.A., Brinksma, E.J., Gleason, J.F., Veefkind, J.P., Cede, A., Herman, J.R., Ionov, D., Goutail, F., Pommereau, J.-P., Lambert, J.-C., van Roozendael, M., Pinardi, G., Wittrock, F., Schonhardt, A., Richter, A., Ibrahim, O.W., Wagner, T., Bojkov, B., Mount, G., Spinei, E., Chen, C.M., Pongetti, T.J., Sander, S.P., Bucsela, E.J., Wenig, M.O., Swart, D.P.J., Volten, H., Kroon, M., Levelt, P.F.: Validation of Ozone Monitoring Instrument nitrogen dioxide columns. *J. Geophys. Res.* **113**, D15815 (2008). doi:[10.1029/2007JD008908](https://doi.org/10.1029/2007JD008908)

Chance, K.: OMI algorithm theoretical basis document volume IV: OMI trace gas algorithms. (2002)

Chatfield, R.B., Esswein, R.F.: Estimation of surface O₃ from lower-troposphere partial-column information: Vertical correlations and covariances in ozonesonde profiles. *Atmospheric Environment* **61**, 103–113 (2012). doi:[10.1016/j.atmosenv.2012.06.033](https://doi.org/10.1016/j.atmosenv.2012.06.033)

Hains, J.C., Folkert Boersma, K., Kroon, M., Dirksen, R.J., Cohen, R.C., Perring, A.E., Bucsela, E., Volten, H., Swart, D.P.J., Richter, A., Wittrock, F., Schoenhardt, A., Wagner, T., Ibrahim, O.W., van Roozendael, M., Pinardi, G., Gleason, J.F., Veefkind, J.P., Levelt, P.: Testing and improving OMI DOMINO tropospheric NO₂ using observations from the DANDELIONS AND INTEX-B validation campaigns. *J. Geophys. Res.* **115**, D05301 (2010). doi:[10.1029/2009JD012399](https://doi.org/10.1029/2009JD012399)

Herman, J., Cede, A., Spinei, E., Mount, G., Tzortziou, M., Abu Hassan, N.: NO₂ column amounts from ground-based Pandora and MFDOAS spectrometers using the direct-sun DOAS technique: Intercomparisons and application to OMI validation. *J. Geophys. Res.* **114**, D13307 (2009). doi:[10.1029/2009JD011848](https://doi.org/10.1029/2009JD011848)

Holben, B.N., Eck, T.F., Slutsker, I., Tanre, D., Buis, J.P., Setzer, A., Vermote, E., Reagan, J.A., Kaufman, Y.J., Nakajima, T., Lavenu, F., Jankowiak, I., Smirnov, A.: AERONET—A federated instrument network and data archive for aerosol characterization. *Remote. Sens. Environ.* **66**(1) (1998). doi:[10.1016/S0034-4257\(98\)00031-5](https://doi.org/10.1016/S0034-4257(98)00031-5)

Hsu, N.C., McPeters, R.D., Seftor, C.J., Thompson, A.M.: The effect of an improved cloud climatology on the TOMS total ozone record. *J. Geophys. Res.* **102**, 4247–4255 (1997)

Ionov, D.V., Timofeyev, Y.M., Sinyakov, V.P., Semenov, V.K., Goutail, F., Pommereau, J.-P., Bucsela, E.J., Celarier, E.A., Kroon, M.: Ground-based validation of EOS-Aura OMI NO₂ vertical column data in the midlatitude mountain ranges of Tien Shan (Kyrgyzstan) and Alps (France). *J. Geophys. Res.* **113**, D15S08 (2008). doi:[10.1029/2007JD008659](https://doi.org/10.1029/2007JD008659)

Knepp, T., Pippin, M., Crawford, J., Chen, G., Szykman, J., Long, R., Cowen, L., Cede, A., Abu Hassan, N., Herman, J., Delgado, R., Compton, J., Berkoff, T., Fishman, J., Martins, D., Stauffer, R., Thompson, A. M., Knapp, D., Montzka, D., Lenscho2, D., Neil, D.: Estimating surface NO₂ and SO₂ mixing ratios from fast-response total column observations and potential application to geostationary missions, submitted for publication for Journal of Atmospheric Chemistry (2012)

Komhyr, W.D.: Electrochemical concentration cells for gas analysis. *Ann. Geophys.* **25**, 203–210 (1969)

Krotkov, N. A., the OMI NO₂ Algorithm Team: OMNO2 README File, 6.2 http://toms.gsfc.nasa.gov/omi/no2/OMNO2_readme_v003.pdf (2012).

Levelt, P.F., van den Oord, G. H. J., Dobber, M. R., Malkki, A., Huib, V., de Vries, J., Stammes, P., Lundell, J. O. V., Saari, H.: The ozone monitoring instrument, *IEEE Transactions on Geoscience and Remote Sensing*, **44** (2006)

Martins, D.K., Stauffer, R.M., Thompson, A.M., Knepp, T.N., Pippin, M.: Surface ozone at a coastal suburban site in 2009 and 2010: Relationships to chemical and meteorological processes. *J. Geophys. Res.* **117**, D05306 (2012). doi:[10.1029/2011JD016828](https://doi.org/10.1029/2011JD016828)

McPeters, R., Kroon, M., Labow, G., Brinksma, E., Balis, D., Petropavlovskikh, I., Veefkind, J.P., Bhartia, P.K., Levelt, P.F.: Validation of the Aura Ozone Monitoring Instrument total column ozone product. *J. Geophys. Res.* **113**, D15S14 (2008). doi:[10.1029/2007JD008802](https://doi.org/10.1029/2007JD008802)

McPeters, R.D., Labow, G.J.: Climatology 2011: An MLS and sonde derived ozone climatology for satellite retrieval algorithms. *J. Geophys. Res.* **117**, D10303 (2012). doi:[10.1029/2011JD017006](https://doi.org/10.1029/2011JD017006)

Piters, A. J. M., Boersma, K. F., Kroon, M., Hains, J. C., van Roozendael, M., Wittrock, F., Abuhassan, N., Adams, C., Akrami, M., Allaart, M. A. F., Apituley, A., Bergwerff, J. B., Berkhouwt, A. J. C., Brunner, D., Cede, A., Chong, J., Clémér, K., Fayt, C., Frieb, U., Gast, L. F. L., Gil-Ojeda, M., Goutail, F., Graves, R., Griesfeller, A., Großmann, K., Hemerijckx, G., Hendrick, F., Henzing, B., Herman, J., Hermans, C., Hoexum, M., van der Hoff, G. R., Irie, H., Johnston, P. V., Kanaya, Y., Kim, Y. J., Klein Baltink, H., Kreher, K., de Leeuw, G., Leigh, R., Merlaud, A., Moerman, M. M., Monks, P. S., Mount, G. H., Navarro-Comas, M., Oetjen, H., Pazmino, A., Perez-Camacho, M., Peters, E., Du Piesanie, A., Pinardi, G., Puentadura, O., Richter, A., Roscoe, H. K., Schönhardt, A., Schwarzenbach, B., Shaiganfar, R., Sluis, W., Spinei, E., Stolk, A. P., Strong, K., Swart, D. P. J., Takashima, H., Vlemmix, T., Vrekoussis, M., Wagner, T., Whyte, C., Wilson, K. M., Yelma, M., Yilmaz, S., Zieger, P., Zhou, Y.: The Cabauw Intercomparison campaign for Nitrogen Dioxide measuring Instruments (CINDI): design, execution, and early results, *Atmospheric Measurement Techniques*, **5** (2012). doi: [10.5194/amt-5-457-2012](https://doi.org/10.5194/amt-5-457-2012)

Remer, L., Kaufman, Y.J., Tanre, D., Mattoe, S., Chu, D.A., Martins, J.V., Li, R.-R., Ichoku, C., Levy, R.C., Kleidman, R.G., Eck, T.F., Vermote, E., Holben, B.N.: The MODIS aerosol algorithm, products, and validation. *J. Atmos. Sci.* **68**, 947–973 (2005). doi:[10.1175/JAS3385.1](https://doi.org/10.1175/JAS3385.1)

Rienecker, M.M., Suarez, M.J., Gelaro, R., Todling, R., Bacmeister, J., Liu, E., Bosilovich, M.G., Schubert, S.D., Takacs, L., Kim, G., Bloom, S., Chen, J., Collins, D., Conaty, A., da Silva, A., Gu, W., Joiner, J., Koster, R.D., Lucchesi, R., Molod, A., Owens, T., Pawson, S., Pegion, P., Redder, C.R., Reichle, R., Robertson, F.R., Ruddick, A.G., Seinkiewicz, M., Woolen, J.: MERRA: NASA's Modern-Era Retrospective Analysis for Research and Applications. *J. Clim.* **24** (2011). doi:[10.1175/JCLI-D-11-00015.1](https://doi.org/10.1175/JCLI-D-11-00015.1)

Savtchenko, A., Ouzounov, D., Ahmad, S., Acker, J., Leptoukh, G., Koziana, J., Nickless, D.: Terra and Aqua MODIS products available from NASA GES DAAC. *Advances in Space Research* **34** (2004). doi:[10.1016/j.asr.2004.03.012](https://doi.org/10.1016/j.asr.2004.03.012)

Schoeberl, M.R., Douglass, A.R., Hilsenrath, E., Bhartia, P.K., Beer, R., Waters, J.W., Gunson, M.R., Froidevaux, L., Gille, J.C., Barnett, J.J., Levelt, P.F., DeCola, P.: Overview of the EOS Aura mission. *IEEE Trans. Geosci. Remote Sens.* **44** (2006). doi:[10.1109/TGRS.2005.861950](https://doi.org/10.1109/TGRS.2005.861950)

Smit, H.G.J., Wolfgang, S., Johnson, B.J., Oltmans, S.J., Davies, J., Tarasick, D.W., Hoegger, B., Stubi, R., Schmidlin, F.J., Northam, T., Thompson, A.M., Witte, J.C., Boyd, I., Posny, F.: Assessment of the performance of ECC-ozonesondes under quasi-flight conditions in the environmental simulation chamber: Insights from the Juelich Ozone Sonde Intercomparison Experiment (JOSIE). *J. Geophys. Res.* **112**, D19306 (2007). doi:[10.1029/2006JD007308](https://doi.org/10.1029/2006JD007308)

Spinhirne, J.D.: Micro Pulse Lidar. *IEEE Trans. Geosci. Remote Sens.* **31**, 1 (1993)

Thompson, A.M., McNamara, D.P., Pickering, K.E., McPeters, R.D.: Effect of marine stratocumulus clouds on TOMS ozone. *J. Geophys. Res.* **98**, 23051–23057 (1993)

Thompson, A.M., Witte, J.C., McPeters, R.D., Oltmans, S.J., Schmidlin, F.J., Logan, J.A., Fujiwara, M., Kirchoff, V.W.J.H., Posny, F., Coetzee, G.J.R., Hoegger, B., Kawakami, S., Ogawa, T., Johnson, B.J., Vomel, H., Labow, G.: Southern hemisphere additional ozonesondes (SHADOZ) 1998–2000 tropical ozone climatology, 1, comparison with Total Ozone Mapping Spectrometer (TOMS) and ground-based measurements. *J. Geophys. Res.* **108**(D2), 8238 (2003). doi:[10.1029/2001JD000967](https://doi.org/10.1029/2001JD000967)

Tzortziou, M., Herman, J.R., Cede, A., Abuhassan, N.: High precision, absolute total column ozone measurements from the Pandora spectrometer system: Comparisons with data from a Brewer double monochromator and Aura OMI. *J. Geophys. Res.* **117**, D16303 (2012). doi:[10.1029/2012JD017814](https://doi.org/10.1029/2012JD017814)

Wang, S., Pongetti, T.J., Sander, S.P., Spinei, E., Mount, G.H., Cede, A., Herman, J.: Direct Sun Measurements of NO₂ column abundances from Table Mountain, California: Intercomparison of low-and high-resolution spectrometers. *J. Geophys. Res.* **115**, D13305 (2010). doi:[10.1029/2009JD013503](https://doi.org/10.1029/2009JD013503)

Wenig, M.O., Cede, A.M., Bucsela, E.J., Celarier, E.A., Boersma, K.F., Veefkind, J.P., Brinksma, E.J., Gleason, J.F., Herman, J.R.: Validation of OMI tropospheric NO₂ Column densities using direct-sun mode brewer measurements at NASA Goddard space flight center. *J. Geophys. Res.* **113** (2008). doi:[10.1029/2007JD008988](https://doi.org/10.1029/2007JD008988)

Yang, K., Bhartia, P. K.: OMTO3 README File. http://disc.sci.gsfc.nasa.gov/Aura/data holdings/OMI/omto3_v003.shtml (2012).